Analysis of Subcarrier and Antenna Power Allocation for MIMO WPMCM System with Sphere Decoder

R.DEEPA
Department of ECE,
Amrita Vishwa Vidhyapeetham,
Ettimadai,
Coimbatore, T.N.,
ecedeepa@gmail.com

Dr.K.Baskaran
Department of ECE,
Government College of Technology,
Coimbatore, T.N.

Abstract: - In order to achieve the efficient usage of the available bandwidth in wireless environments, the best method for real time application would be combining Multi- Input Multi-Output (MIMO) and Orthogonal Frequency Division Multiplexing (OFDM) with Cyclic Prefix (CP) together. The OFDM implemented by using IFFT's and FFT's have major drawbacks like ISI (intersymbol interference), Time and Frequency Synchronization and Carrier Frequency Offset. To alleviate the above problems wavelet transform is used to generate the orthogonal carrier. This paper investigates joint subcarrier and antenna power allocation in WPMCM system. The transmit (antenna) power is allocated for the proposed combination using the Lagrangian method and compared with the conventional power allocation scheme. Existing sub-optimal techniques either use equal power allocation and perform only subcarrier allocation or handle subcarrier and power allocation separately. In this paper, we propose an algorithm that performs joint subcarrier and power allocation to reduce the BER under a total power constraint.

Key-Words: - MIMO-WPMCM, antenna, sub-carrier power allocation, sphere decoder

1 Introduction

One of the several forms of Smart Antenna Technology is the use of multiple antennas at both the transmitter and receiver to improve the system performance. MIMO gives significant increase in data transmission without additional bandwidth or transmit power [1]. MIMO transmits and receives two or more data streams through a single radio channel. This means the system can deliver two or more times the data rate per channel. By allowing this multiple streaming, wireless data capacity is multiplied without any additional frequency spectrum. Some of the standards like IEEE 802.11n, 4G and IEEE 802.11 Wireless LAN standards use MIMO technology.

OFDM uses the spectrum efficiently by spacing its carriers as close as possible. This is enabled by constructing orthogonal carriers. Since OFDM can overcome the effect of multipath fading by using a guard period, OFDM needs only a simple equalization method in combating selective fading channels [2]. Standards like 802.11a and 802.11g systems use OFDM. It provides reliable transmission in Mobile Radio Communication [3],[5],[12],3G, WiBro, WiMAX, 802.20 and 4G standards use MIMO OFDM. It effectively uses the multipath fading channel and improves the bandwidth effectively. The power for the transmit antennas is allocated, using the Lagrangian optimization and the combined greedy algorithm method, for the best performing detection scheme.

Resource allocation techniques for multiuser Orthogonal Frequency Division Multiplexing (OFDM) are of two types: fixed [4] and dynamic [7], [9], [16], [18]. Fixed resource allocation techniques fail to exploit multiuser diversity resulting in poor system performance. On the other hand, dynamic resource allocation techniques allocate resources (subcarriers and time slots) taking into account the users' current channel conditions.

In image and video transmission applications, several approaches have been proposed to improve the robustness of image and video transmission over error-prone network such as

Internet and wireless network. Conventional OFDM/QAM systems are robust for multi-path channels due to the cyclically prefixed guard interval which is inserted between consequent symbols to cancel ISI. However, this guard interval decreases the spectral efficiency of the OFDM system as the corresponding amount [11]. Thus, there have been approaches of wavelet-based OFDM which does not require the use of the guard interval. It is found that OFDM based on Haar orthonormal wavelets (DWT-OFDM) are capable of reducing the ISI and ICI, which are caused by the loss in orthogonality between the carriers[14]-[15].

The multiuser MIMO-OFDM system has great potential of providing enormous capacity due to its integrated space-frequency diversity and multiuser diversity. Assuming that the knowledge of channel state information (CSI) is available at the transmitter, the performance can be further improved through the adaptive resource allocation. For the OFDMA systems with single antenna, several resource allocation methods were proposed in literature to minimize the total transmit power given QoS by utilizing the multiuser diversity in frequency domain.

In Section II, the MIMO WPMCM system is defined. The sphere detection algorithm is described in Section III and Section IV deals with the power allocation scheme proposed. In Section V, the experimental results are validated and in Section VI, the conclusions are discussed.

2 System Description

2.1 Transmitter (Vertically Layered)

The proposed model is given in figure 1. The MIMO system utilizes multiple transmit (N_t) and receive (N_r) antennas to exploit the spatial multiplexing gain provided by inherent orthogonality severe multipath-channels. The transmission sequence is modulated using Quadrature Amplitude Modulation (QAM) and demultiplexed (serial-to-parallel conversion) into N_t independent parallel streams, each of which is assigned to each transmit-antenna. Such a scheme results in a vertically-layered sequence of data, that is to be interpreted at the receiver. The transmission at the k^{th} OFDM symbol-period is analytically represented as

$$r_k = H_k\ c_k + n_k \tag{1}$$

where c denotes the $N_t \times 1$ transmitted vector $c = [c_1,c_2,\ldots,c_{Nt}]^T$, r denotes the $N_r \times 1$ received vector $r = [r_1,r_2,\ldots,r_{Nr}]^T$, n denotes $N_r \times 1$ additive white gaussian noise (AWGN) vector (*N(0,1)*) and H denotes the $N_r \times N_t$ channel matrix $[h_{ij}]_{Nr \times Nt}$, assumed to represent an i.i.d. Rayleigh quasi-static (constant during one OFDM symbol) and flat-fading channel, each element of which is a circularly symmetric zero-mean unit-variance Gaussian random variable representing the complex gain between the respective transmit and receive antennas.

2.2 DWT based MIMO-OFDM

The conventional OFDM includes IFFT at the transmitter and FFT at the receiver. The block divides the incoming symbol-stream into blocks of size N, denoting the number of subcarriers in the OFDM symbol, and modulates each subcarrier with each symbol using an N-point IFFT operation, Fig.2. This is followed by a parallel-to-serial conversion of the data, addition of a cyclic prefix and transmission. Also, the transmission of independent data using orthogonally separated carriers further enhances the multiplexing gain provided by the MIMO system. This creates a system, wherein, even in wideband situations (frequency – selective channels), the OFDM separates the frequency selective channels into independent and parallel narrowband (flat fading) channels. The inverse of these operations are performed at the receiver side as shown in Figure 3.This means that the MIMO-OFDM system can be interpreted as N separate spatial multiplexing systems, where for the p^{th} tone (subcarrier).

$$r_p = H_p\ c_p + n_p \tag{2}$$

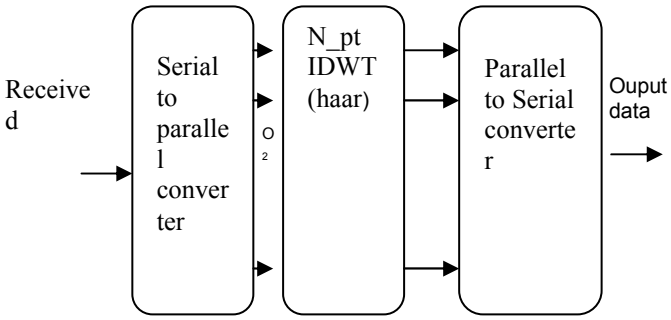

Figure 2. IDWT based OFDM Module

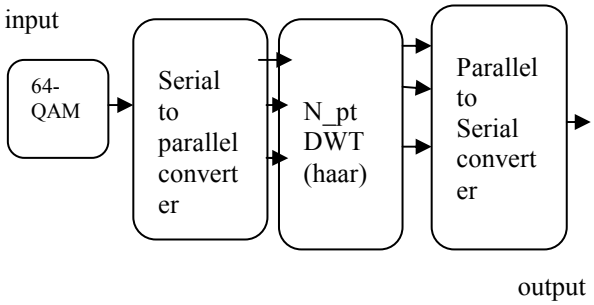

Figure 3. DWT based Inverse OFDM Module

2.3 Forward Transform

The wavelet and scaling functions are calculated as

$$a(k)_j = \sum_m h(2m \quad k)a(m)_{j+1} \tag{3}$$

$$b(k)_j = \sum_m g(2m \quad k)b(m)_{j+1} \tag{4}$$

where *h* and *g* are low-pass and high-pass filters corresponding to the coefficients *h(k)* and *g(k)* respectively. The down- arrow denotes a decimation or down-sampling by two. The transformation matrix is as given below:

$$\begin{matrix} h_0 & h_1 & 0 & 0 & \cdots \\ g_0 & g_1 & 0 & 0 & \cdots \\ 0 & 0 & h_0 & h_1 & \cdots \\ 0 & 0 & g_0 & g_1 & \cdots \\ \vdots & \vdots & \vdots & \vdots & \ddots \end{matrix}$$

The first step of the forward Haar transform for an eight element signal is shown below. Here signal is multiplied by the forward transform matrix.

$$\begin{bmatrix} a_0 \\ a_1 \\ a_2 \\ a_3 \\ c_0 \\ c_1 \\ c_2 \\ c_3 \end{bmatrix} = \begin{bmatrix} \frac{1}{2} & \frac{1}{2} & 0 & 0 & 0 & 0 & 0 & 0 \\ \frac{1}{2} & -\frac{1}{2} & 0 & 0 & 0 & 0 & 0 & 0 \\ 0 & 0 & \frac{1}{2} & \frac{1}{2} & 0 & 0 & 0 & 0 \\ 0 & 0 & \frac{1}{2} & -\frac{1}{2} & 0 & 0 & 0 & 0 \\ 0 & 0 & 0 & 0 & \frac{1}{2} & \frac{1}{2} & 0 & 0 \\ 0 & 0 & 0 & 0 & \frac{1}{2} & -\frac{1}{2} & 0 & 0 \\ 0 & 0 & 0 & 0 & 0 & 0 & \frac{1}{2} & \frac{1}{2} \\ 0 & 0 & 0 & 0 & 0 & 0 & \frac{1}{2} & -\frac{1}{2} \end{bmatrix} \bullet \begin{bmatrix} s_0 \\ s_1 \\ s_2 \\ s_3 \\ s_4 \\ s_5 \\ s_6 \\ s_7 \end{bmatrix}$$

2.4 Inverse Transform

Like the forward Haar transform, a step in the inverse Haar transform is described in linear algebra terms. The matrix operation to reverse the first step of the Haar transform for an eight element signal is shown below.

$$\begin{bmatrix} s_0 \\ s_1 \\ s_2 \\ s_3 \\ s_4 \\ s_5 \\ s_6 \\ s_7 \end{bmatrix} = \begin{bmatrix} 1 & 1 & 0 & 0 & 0 & 0 & 0 & 0 \\ 1 & -1 & 0 & 0 & 0 & 0 & 0 & 0 \\ 0 & 0 & 1 & 1 & 0 & 0 & 0 & 0 \\ 0 & 0 & 1 & -1 & 0 & 0 & 0 & 0 \\ 0 & 0 & 0 & 0 & 1 & 1 & 0 & 0 \\ 0 & 0 & 0 & 0 & 1 & -1 & 0 & 0 \\ 0 & 0 & 0 & 0 & 0 & 0 & 1 & 1 \\ 0 & 0 & 0 & 0 & 0 & 0 & 1 & -1 \end{bmatrix} \bullet \begin{bmatrix} a_0 \\ a_1 \\ a_2 \\ a_3 \\ c_0 \\ c_1 \\ c_2 \\ c_3 \end{bmatrix}$$

The wavelet transform is a transform similar to the Fourier transform with a completely different merit function. Fourier transform decomposes the signal into sines and cosines, i.e. the functions are localized in Fourier space; in contrary the wavelet transform uses functions that are localized in both the real and Fourier space. Generally, the wavelet transform can be expressed by the following equation:

$$F(a,b) = \int_{-\infty}^{\infty} f(x)\, \psi^*_{(a,b)}(x)\, \mathrm{d}x \tag{5}$$

where the * is the complex conjugate symbol and function ψ is some function.

The wavelet can be constructed from a scaling function which describes its scaling properties. The restriction that the scaling functions must be orthogonal to its discrete translations implies some mathematical conditions on them which are mentioned everywhere, e.g. the dilation equation

$$\phi(x) = \sum_{k=-\infty}^{\infty} a_k \phi(Sx - k) \quad (6)$$

where S, a scaling factor is usually chosen as 2 and is shown in figure 4. Moreover, the area between the function must be normalized and scaling function must be orthogonal to its integer translates.

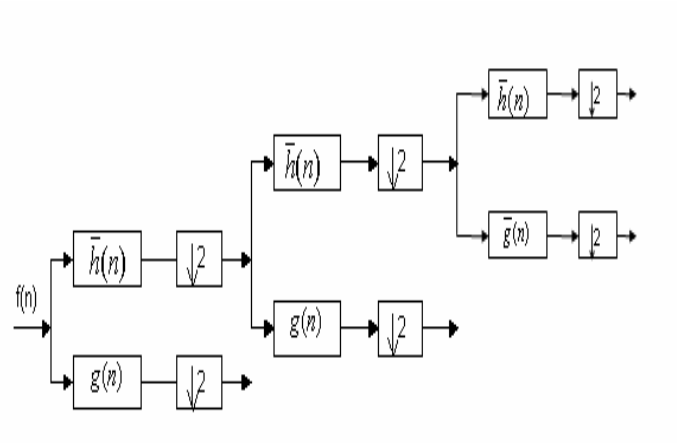

Figure 4: Structure of wavelet decomposition

3 Decoding Algorithm- Sphere Decoder

The received vector can be written as,

$$R = H s + n \quad (7)$$

The maximum likelihood decoding algorithm is given by:

$$\|c\|^2 = \|y - Ax\|^2 = (x - \hat{x})^* A^* A(x - \hat{x}) + \|y\|^2 - \|A\hat{x}\|^2, \quad (8)$$

where $\hat{x}$ is the unconstrained maximum likelihood estimate of x, and defined as

$$\hat{x} = A^{\dagger} y = (A^T A)^{-1} A^T y \quad (9)$$

Rewrite the maximum likelihood metric as follows:

$$\hat{x}_{ML} = \text{argmin} \ \|y - Ax\|^2 \ x \in S \quad (10)$$

$$= \text{argmin} \quad (x - \hat{x})^* A^* A(x - \hat{x}) \ ; \ x \in S.$$

A lattice point which lies inside the sphere with radius d has to fulfil the condition

$$d^2 \geq \|c\|^2 \quad (11)$$

A new constant can be defined as $d'^2 = d^2 - \|y\|^2 + \|A\hat{x}\|^2$, and can be rewritten as

$$d'^2 \geq (x - \hat{x})^* A^* A(x - \hat{x}) \quad (12)$$

The matrix A*A can be decomposed to triangular matrices with Cholesky decomposition (A*A = U*U), where U is an upper triangular matrix

$$U = \begin{bmatrix} u_{11} & u_{12} & \cdots & u_{1n-1} & u_{1n} \\ 0 & \vdots & \ddots & u_{2n-1} & \vdots \\ 0 & 0 & \cdots & 0 & u_{mn} \end{bmatrix} \quad (13)$$

where $u_{i,j}$ denotes element (i, j) of the matrix U. Further simplification gives

$$d'^2 \geq (x - \hat{x})^* A^* A(x - \hat{x})$$

$$= (x - \hat{x})^* U^* U(x - \hat{x})$$

$$= \sum_{i=1}^{Q} u_{i,i}^2 \left((x_i - \hat{x}_i) + \sum_{j=i+1}^{Q} \frac{u_{i,j}}{u_{i,i}} (x_j - - \hat{x}_j)\right)^2 \quad (14)$$

Because of the upper triangular nature of U,

one can begin evaluation of the last element in x as

$$u_{Q,Q}^2(x_Q - \hat{x}_Q)^2 \leq d'^2 \quad (15)$$

which leads to

$$\left\lceil \hat{x}_Q - \frac{d'}{u_{Q,Q}} \right\rceil \leq x_Q \leq \left\lfloor \hat{x}_Q + \frac{d'}{u_{Q,Q}} \right\rfloor \quad (16)$$

where ⌈a⌉ rounds to the nearest symbol value greater than or equal to a. Similarly ⌊a⌋ rounds to the nearest symbol value less than or equal to a. In a similar fashion, one proceeds for x_{Q-2}, and so on, stating nested necessary conditions for all elements of x. To ensure that the lattice point is inside the sphere, the initial radius must be big enough to enclose at least one lattice point. One method is to use statistical properties of the signal. Note that $\|c\|^2/\sigma^2 v$ has a Chi-Square distribution with 2NL degrees of freedom, since each entry of the noise is an independent N (0, σ2 v) random variable. The probability of the lattice point inside the sphere can be written as

$$Pr\left[\|b\|^2 \leq d^2\right] = \Pr\left[\frac{\|b\|^2}{\sigma_v^2} \leq \frac{d^2}{\sigma_v^2}\right] \quad (17)$$

Where

$\Gamma(NL) = \int_0^\infty t^{NL-1} e^{-t}\, dt$

Out of the two most commonly used tree search strategies, Fincke- Pohst and Schnorr Euchner, the latter is the most preferred one which is practically easy to implement. Hardware implementation of lattice decoding algorithms becomes a challenging task as the complexity of the MIMO systems increases. The design and implementation of a Schnorr Euchner strategy based lattice decoder is done using HDL Coder and FPGA. This lattice decoding algorithm has high data dependency during the iterative closest lattice point search procedures. The parallelism of the algorithm is explored and efficient hardware architectures are developed with the decoding function on FPGA and the data pre processing on DSP.

Considering the complexity of the algorithm, MIMO decoders are generally implemented using DSPs, such as Bell Labs layered space-time (BLAST) system. Field programmable gate arrays (FPGAs) are widely used in signal processing because of their reconfigurability and the support of parallelism. Even the developing cycle is longer than DSP implementation, once an efficient architecture is developed and the parallelism of the algorithm is explored, FPGAs can be used to significantly improve the processing speed of signal processing or wireless communication systems. The successful implementation of Viterbi decoder and Turbo decoder has proved the power of FPGA. The analysis of the lattice decoder algorithm for hardware realization is the main purpose. The AV algorithm is examined and the data dependency for parallel implementation is analyzed. The structure of this algorithm is developed, and is prototyped on Xilinx ISE 11.1.

Considering a MIMO-WPMCM system with *M* transmit and *N* receive antennas, the received signal ***r*** is rewritten as

$$r = H s + n \quad (18)$$

where ***s*** denotes the transmitted vector, and *n* is a *N* ×1 random vector of white Gaussian noise. *H* is an *N* ×*M* channel transfer matrix, which generates the lattice. The flowchart of the sphere decoding algorithm has been described in detail in Figure 13.

Each time the algorithm finds a k-dimensional layer, the distance to which is less than the currently smallest distance, this layer is expanded into (k-1) -dimensional sub layers. This is done in Case A. Conversely, as soon as the distance to the examined layer is greater than the lowest distance, the algorithm moves up one step in the hierarchy of layers (Case C).

Case B is invoked when the algorithm has successfully moved down all the way to the zero-dimensional layer (that is, a lattice point) without exceeding the lowest distance. Then this lattice point is stored as a potential output point, the lowest distance is updated, and the algorithm moves back up again, without restarting.

The pre processing stage involves matrix inversion and QR decomposition operations, therefore DSP is chosen to compute the lower-triangular matrix ***G*** and is responsible for data transport of input and output through the I/O interface. The input and output buffers are implemented using two external single port SRAMs, and register arrays are created in the FPGA to temporally store the data during the lattice point search procedure. A finite state machine (FSM) is designed as the decoder controller to organize the closest point search algorithm and to synchronize the operations between functional blocks. Three parameters the Euclidean distance d_{new} to the currently investigated layer of the lattice, the currently smallest distance d_{best}, and the index k ($1 \le k \le N$), determine the state transitions.

4 Power allocation scheme

Case (i): Antenna Power Allocation:

When the transmit power is equally shared in the space domain, the global power is not optimized. Lagrangian method evaluated on the BER expression is used for obtaining the optimal transmit power. The power allocation is obtained by using the estimate value of the BER. The power allocation is obtained by using the estimate value of the BER. The generalized expression for BER (for BPSK modulation) can be determined as:

$$g(\sigma_l, p_l) \approx p \times \exp\{-q \times \sigma_l \times p_l\} \tag{19}$$

where

$$\sigma_l = \frac{1}{(2^m - 1).\sigma_n^2 \sum_{n=0}^{N_r-1} \left| w^{(l,n)} \right|^2} \tag{20}$$

The transmit power for the l-th transmit antenna is denoted as p_l and m is the number of bits used for representing a modulated symbol. The constraint used for obtaining the Lagrangian solution is:

$$\sum_{l=0}^{N_t-1} p_l - N_t.P_a = 0 \tag{21}$$

where P_a is the average power transmitted by the antennas. The Lagrangian method is evaluated for the following:

$$F(p_1,...,p_N) = \frac{1}{N_t} \sum_{l=0} g(\sigma_l, p_l) + \lambda \times \left(\sum_{l=0}^{N_t-1} p_l - N_t \times P_a \right) \tag{22}$$

where λ is the Lagrangian multiplier.For each transmit antenna, the above expression is solved to get the optimal solutions.

$$\begin{aligned} &\frac{1}{N_t} . \frac{\partial}{\partial p_l} \left(\sum_{l=0}^{N_t-1} g(\sigma_l, p_l) \right) + \lambda = 0 \\ &\sum_{l=0}^{N_t-1} p_l - N_t.P_a = 0 \end{aligned} \tag{23}$$

By using BER estimation in the above equation we obtain the following

$$\begin{aligned} &\frac{(-p.q.\sigma_l)}{N_t} \times \exp(-q.\sigma_l.p_l) + \lambda = 0 \\ &\sum_{l=0}^{N_t-1} p_l - N_t.P_a = 0 \end{aligned} \tag{24}$$

Finally the general solution obtained is:

$$F(p_1,...,p_N) = \frac{1}{N_t} \sum_{l=0} g(\sigma_l, p_l) + \lambda \times \left(\sum_{l=0}^{N_t-1} p_l - N_t \times P_a \right) \tag{25}$$

Henceforth for Unequal Power Allocation (UPA), the solution obtained in (24) is used. It is recommended to allocate power according to the conventional scheme or Equal Power Allocation (EPA) when a solution say $p_l \le 0$ is obtained.

Case (ii) Bit and Power allocation for Sub-Carriers Greedy algorithm

Under the constraint of given bit rate and the target BER requirement, this method can adaptively adjust the transmit power of each sub-carrier to minimize the transmit power of the system. Different bits and modulations are allocated for each sub-carrier according to the channel state of each sub-carrier. Since the power needed for transmitting definite bits is independent of each other, it is approved that the optimal bit allocation is greedy allocation. Dynamic bit and power allocation strategy based on greedy algorithm is followed, that is, in this algorithm, *m* bits are allocated to sub-carrier, each time it selects the sub-carrier for which transmission of *m* additional bit can be done with the smallest additional transmit power for a request BER. It can be formulated as follows

1) Algorithm Initialization

- let $c_n = 0$,n= 1, 2,…,N;
- decide step m ;
- Compute $\Delta P_n = [f(m) - f(0)]/\alpha_n^2$.

2) Bit Allocation

- find the bit that will cost the least to increment $\Delta P_n = [f(m) - f(0)]/\alpha_n^2$
- choose the sub-carrier which index is $\hat{n} = \arg\min P_{n\hat{}}$.
- allocate the sub-carrier m bit, $n\hat{} \; c_{n\hat{}} = c_{n\hat{}} + m$;
- Compute the incremental power of that sub-carrier, $\Delta Pn = [f(c_{n\hat{}} + m) - f(c_{n\hat{}})]/ \alpha_n^2$ again, repeat the above steps R/m time.

3) Results

- $\{c_1, c_2, \ldots c_N\}$ Computed from the above steps is the last bit allocation scheme.
- Power allocation can be denoted as

$$e_n = \frac{2^{c_n} - 1}{SNR_n / GAP}$$

where GAP is a variable parameter.

5 Experimental Results and Discussions

MIMO-WPMCM spatial multiplexing system is employed to simulate the performance and allocate the power using Lagrangian and Greedy algorithm. The Bit Error Ratio, BER, variation for different values of Signal to Noise Ratio, SNR, is plotted in the graphs. The main simulation parameters are tabulated in Table I.

Table I: Simulation Parameters:

Transmitters	Variable
Receivers	Variable
Data subcarriers	1024
Subcarrier spacing	312.5 kHz
Sampling frequency	20 MHz
Channel spacing	20 MHz
Data rate	64 Mbps

The figure 5 shows the results for a two transmitter and two receiver antenna (2x2) system and (4 x 4) is plotted in Figure 6. From this, it is evident that VBLAST/MMSE/MAP (VMM) offers better Bit Error Ratio (BER) performance in comparison with the other detection schemes. Figure 7 shows the superiority of sphere decoder over VBLAST combos. At an SNR of 12 dB, VBLAST combos provide an error rate of 10^{-3}, whereas MAP and sphere decoder require an SNR of only 6 dB for the same performance. The comparison of the algorithms in terms of their BER is done with the plot obtained from MATLAB. From the BER plot obtained its well evident that SD performs almost similar to that of ML with reduced complexity (mathematical computations reduced) and ML performs much better when compared to other existing schemes.

The proposed system makes use of the best available detection scheme. Sphere decoder has been employed at the receiver end. The subcarrier bit and power allocation is achieved by using Greedy algorithm. This is done for the OFDM subcarrier set for each of the MIMO transmitter antennas. Again power allocated to

each of the transmit antennas is achieved by Lagrangian method.

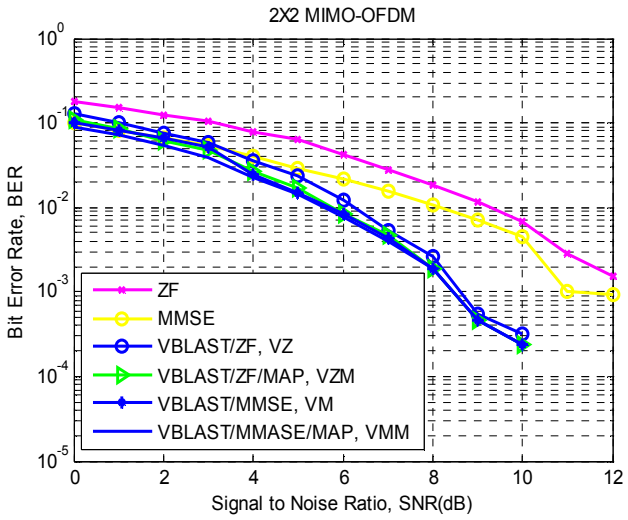

Figure 5 Error plot of 2 X 2 MIMO-OFDM systems

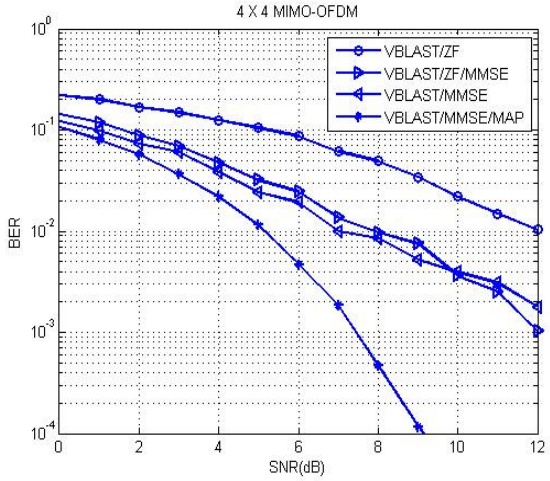

Figure 6 Error plot of 4 X 4 MIMO-OFDM systems

Unequal bit allocation across the sub-carriers helps us to achieve variable transmission rate. The overall power required for data transmission is reduced significantly when this system is employed. The transmitted data is detected at the receiver more efficiently by adapting the proposed detection scheme. The simulation of an OFDM and WPMCM (Haar (db1) Wavelet) system is done for 1024 bits and their respective BER vs SNR curves are plotted and compared in Figure 8. It is observed that BER of 10^{-3} is achieved at around 8 dB for WPMCM system, whereas it is achieved at 18 dB for an OFDM system. Thus, WPMCM system has more than twice SNR improvement. Now, the power is allocated for the transmitter antennas of the 2x2 MIMO OFDM system can be analysed. For Equal (Conventional) Power Allocation (EPA), 1 W is considered as the power for each antenna. The Unequal Power Allocation (UPA) is implemented using the Lagrangian solution and the BER plot is given in Figure 9 .At a particular SNR value, say at SNR=6dB, the Bit Error Ratio (BER) values for the 2x2 and 4x4 configuration is compared in Table II.

The Bit Allocation using Greedy algorithm is done based on the CSI values. Figure 10 and 11 show unequal and equal distribution of 256 bits across 64 Sub-Carriers.

Table II:BER comparison of 2x2 and 4x4 MIMO OFDM Systems for Antenna Power Allocation

Antenna Power Allocation Scheme	**BER of 2x2 system**	**BER of 4x4 system**
Equal (1W)	0.0545	0.0284
Unequal (Lagrangian)	0.0248	0.0117
Unequal (Combined Greedy and Lagrangian)	0.0018	0.0002

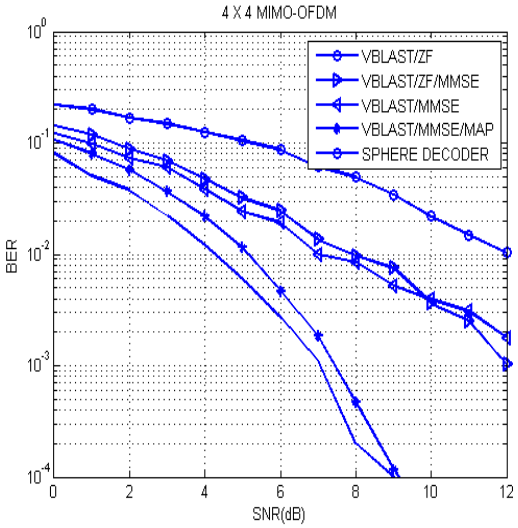

Figure 7 Error plot for 4 x 4 with sphere decoder

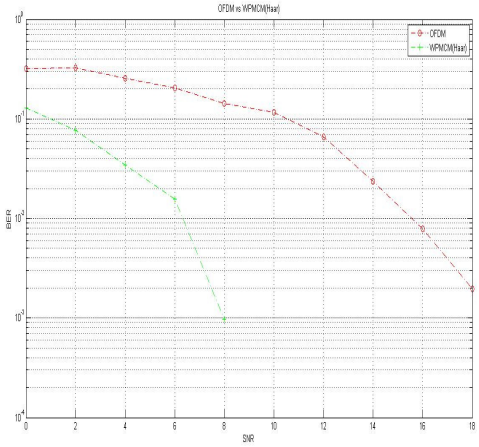

Figure 8 Comparison of OFDM and WPMCM System

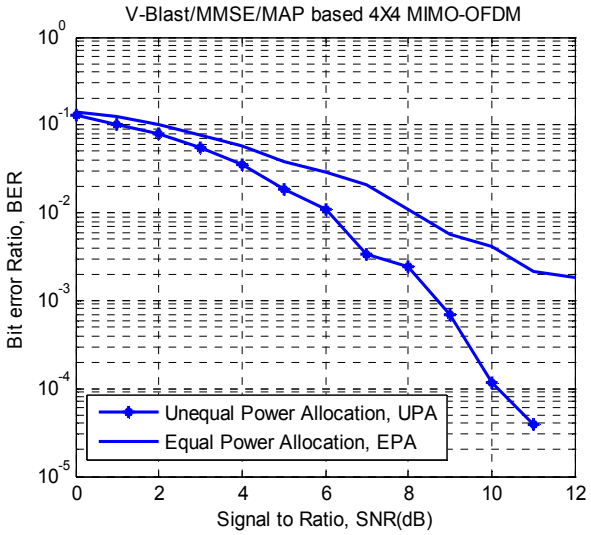

Figure 9: BER performance for Equal and Unequal Antenna Power Allocation for 4x4 system

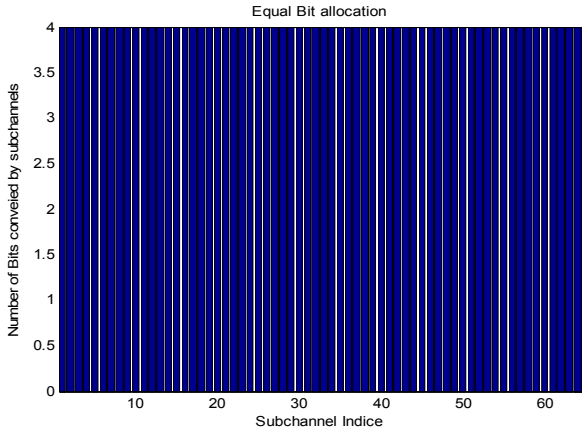

Figure 10: Equal Bit Allocation of 256 bits across 64 Sub-Carriers

Sphere decoder achieves superior Bit Error Rates while retaining the low-complexity nature of the V-BLAST and the error performance of Sphere decoder is close to MLD with reduced complexity. The comparison between the Lagrangian Antenna Power Allocation and Combined Greedy algorithm is analysed for the above proposed scheme (Figure 12). The Combined Greedy outperforms UPA-Lagrangian in the aspect of transmission error reduction.

References:

[1] Theodre Rappaport, Wireless Communication, 2nd edition, *Prentice Hall*, 2002.

[2] John G. Proakis, Masoud Salehi, Communication Systems, 3rd edition, *Pearson Education*, 2005

[3] Auda M. Elshokry, Thesis, "Complexity and Performance Evaluation of Detection Schemes for Spatial Multiplexing MIMO Systems", January 2010.

[4] Toshiaki Koike-Akino, "Low-Complexity Systolic V-BLAST Architecture", *IEEE Transactions on Wireless Communications*, Vol. 8, No. 5, May 2009.

[5] Yavuz Yapici, Thesis, "V-BLAST/MAP: A New Symbol Detection Algorithm for MIMO Channels", January 2005.

[6] Simon Haykins, Communication Systems, 4th edition, *John Wiley & Sons*, Inc., 2001.

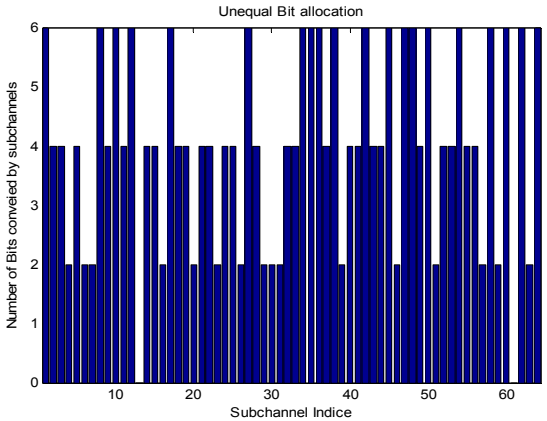

Figure 11: Unequal Bit Allocation (using Greedy algorithm) of 256 bits across 64 Sub-Carriers

[7] Neng Wang and Steven D. Blostein, "Approximate Minimum BER Power Allocation for MIMO spatial multiplexing systems", *IEEE Transactions on Communications*, Vol. 55, No. 1,

January 2007.
[8] Arogyaswami Paulraj, Rohit Nabar, Dhananjay Gore, "Introduction to Space-time Wireless Communication Systems",1st edition, *Cambridge University Press*, 2003.
[9] Wladmir Bocquet, Kazunori Hayashi and Hideaki Sakai, "A Power Allocation Scheme for MIMO OFDM Systems", *IEEE ISCSSP Morocco*, March, 2006.
[10] P.W. Wolnaisky, G.J. Foschini, G.D. Golden, and R.A. Valenzuela,"V-BLAST: an architecture for rich-scattering wireless channel," *URSI International Symposium on Signals and Systems and Electronics*, pp.295-300, 29 Sep-2 Oct 1998.
[11] Teddy Purnamirza, Thesis, "The performance of OFDM in Mobile Radio Channel.", April 2005.
[12] Y. Ding, T. N. Davidson, Z.-Q. Luo, and K. M. Wong, "Minimum BER block precoders for zero-forcing equalization," *IEEE Trans. Signal Process*., vol. 51, no. 9, pp. 2410–2423, Sep. 2003.

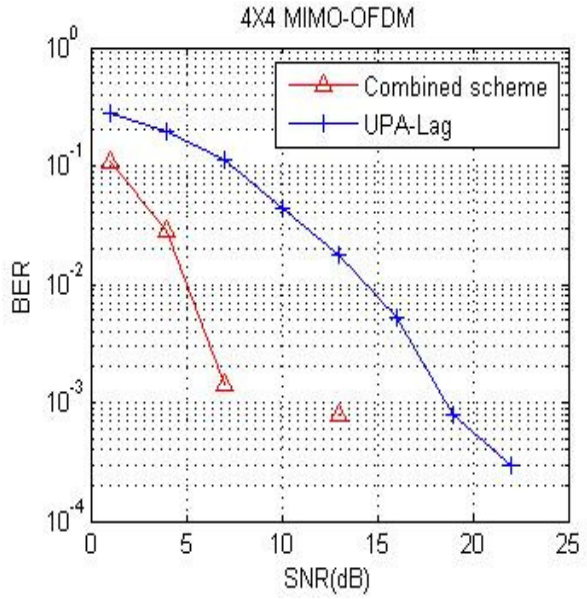

Figure 12:BER performance using Lagrangian and Combined greedy method

[13] C. Y. Wong, R. S. Cheng, K. B. Letaief, and R. D. Murch, "Multiuser OFDM with adaptive subcarrier, bit, and power allocation," *IEEE J.Select. Areas Commun.*, vol. 17, pp. 1747-1758, Oct. 1999.
[14] J. Jang and K. B. Lee, "Transmit power adaptation for multiuser OFDM systems," *IEEE J. Select. Areas Commun.*, vol. 21, pp. 171-178, Feb.2003.
[15] W. Rhee and J. M. Cioffi, "Increase in capacity of multiuser OFDM system using dynamic sub- channel allocation," in *Proc. 51st IEEE VehicularTechnology Conference*, vol. 2, pp. 1085-1089, Spring 2000.
[16] Z. Shen, J. G. Andrews, and B. L. Evans, "Adaptive resource allocation in multiuser OFDM systems with proportional fairness," to appear in *IEEE Trans. Wireless Commun.*
[17] E. Lawrey, "Multiuser OFDM," in *Proc. IEEE International Symposiumon Signal Processing and its Applications*, vol. 2, pp. 761- 764, Aug.1999.
[18] T. L. Tung and K. Yao, "Channel estimation and optimal power allocation for a multiple-antenna OFDM system," *EURASIP J. Applied Signal Processing*, vol. 2002, pp. 330-339, Mar. 2002

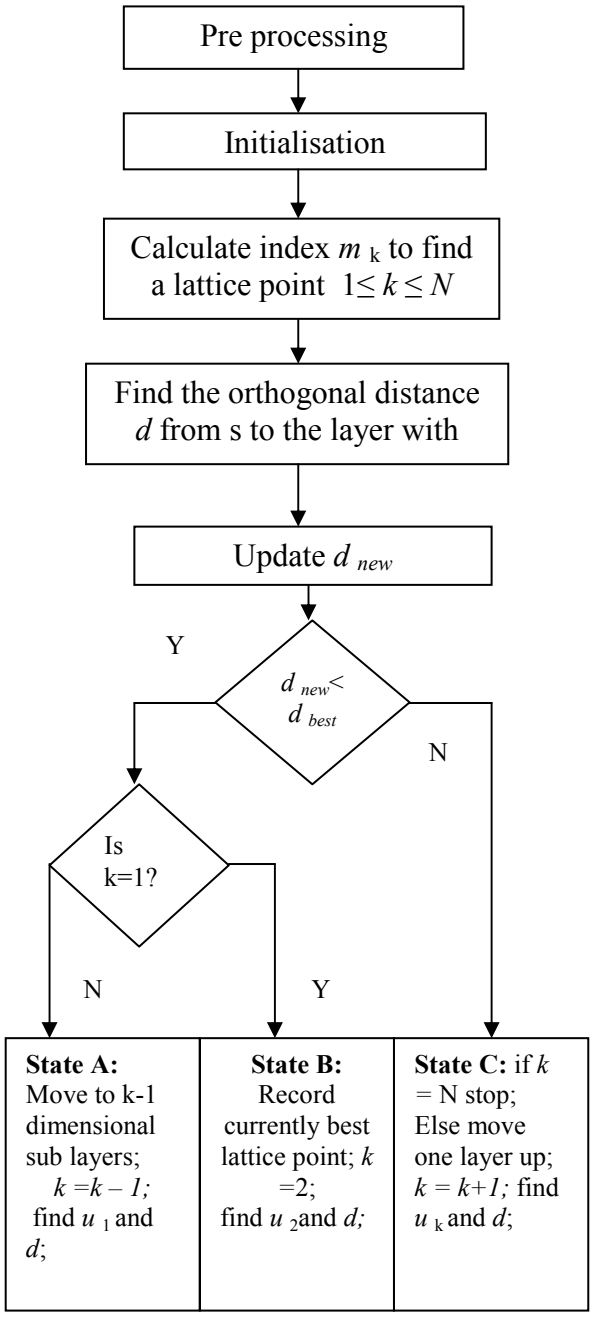

Figure 13 Flowchart of the algorithm

R.Deepa is working as an Assistant Professor in the department of ECE, Amrita Vishwa Vidyapeetham, Coimbatore. Her research areas include MIMO wireless communication, modulation, coding and signal processing. She is a member of IETE and ISTE.

Dr.K.Baskaran is with the Department of Computer Science Engineering in Government College of Technology, Coimbatore. He is a member of IEEE, ISTE and his research areas include mobile computing and wireless communication.